

THE INFLUENCE OF GRAIN SIZE DISTRIBUTION OF PA12 ON KEY STEPS OF THE POLYMER LASER SINTERING PROCESS

Jens P.W. Sessege^{a,b,*}, Paul Riedmann^{a,c}, Sybille Fischer^a, Hans-Joachim Schmid^b

^a EOS GmbH, Robert-Stirling-Ring 1, 82152 Krailling, Germany

^b Paderborn Institute for Additive Fabrication, University of Paderborn, Pohlweg 55, 33098 Paderborn, Germany

^c Department of Mechanical Engineering, Technical University of Munich, Boltzmannstrasse 15, 85748 Garching, Germany

Abstract

As the industry pushes for higher resolution laser sintering, finer and finer powders are required. Yet, this also changes the way powders behave during the process. In this project, the influence of finer particles on the dosing and coating process during laser sintering is being investigated. PA12 laser sintering powder without flow additives was sieved to four fractions with grain sizes with a d_{50} of 42, 54, 61 and 66 μm . These fractions were characterized regarding powder flowability by FT4 powder rheometer. The dosing and coating behavior of these fractions was tested in separate experiments on an EOS P395, where the coating experiments were performed at both RT and 175°C. Furthermore, test jobs were built with the different powder fractions. The larger portion of fines in the finest fraction dominated the powder properties and led to significantly worse powder behavior during the dosing and coating steps, as predicted by analytical measurements.

Keywords

Additive Manufacturing, Laser sintering, Polymer, Grain Size Distribution, Powder Rheology, Polyamide 12

Introduction

Laser sintering is an uprising technology with an expanding range of applications, but also a lot of untapped potential. One direction in which it is being improved, is a finer resolution, which at some point inevitably leads to the topic of finer powders. Finer powders have two advantages that can help improve part quality. One advantage is, that it allows for a thinner layer thickness. This directly impacts the resolution in Z-direction, as it can make the stepping effect of sloped surfaces finer. The other one is the positive influence on the surface quality [1]. Unfortunately, a finer particle distribution, among other parameters, also leads to decreased powder flow properties [2-8]. Good powder flowability is essential for laser sintering. Primarily, the dosing and coating steps need to be ensured. If one of these steps fails, no parts are being built or part quality is compromised. Additionally, powders with better flow properties pack more efficiently, which was shown to positively contribute to better mechanical properties [2] and surface quality [9]. Unfortunately, powder flow cannot be described as a single value, as a powder behaves differently under different conditions. Powders can have significantly different behavior depending on the stress state and whether they are evaluated under static or dynamic conditions [3]. Hence, a powder

that can be easily dosed, may show difficulties in the coating process. Yet, both are required in order to create a decent powder bed.

The theoretical maximum packing density is independent of a spheres' diameter and the material. But it can be improved by a mixture of differently sized particles where smaller particles fill the voids created by densely packed larger particles. In theory, a packing density of near 100% could be reached this way [10]. This would require a multimodal powder with particle sizes ranging over many orders of magnitude. Practically, this kind of powder would be quite difficult to produce and would probably have terrible flow properties. With the currently most common layer thicknesses of 100 to 120 μm , the upper particle size is roughly limited by that value while the lower limit is roughly given by the particle size, when fine particles make the powder too adhesive, a size ratio of 1:3 is probably the limit of what could be expected as grain size difference. Karapatis *et al.* [11] tested the increase in layer density for bimodal metal powders with different concentrations. A 1:2 ratio did not result in a significant improvement, while with a 1:5 ratio an increase in layer density from about 55% to 61% was found. They also found that curves for bulk and layer density are similar, indicating that the same processes occurred, although with less efficiency in the layer case. Nevertheless, it should be kept in mind that Karapatis tested metal powders, while this study investigates polymer powders. The difference in material selection might cause a difference, as the flowability depends of the ratio between adhesion and gravitational forces. Therefore, the effect is most likely less pronounced for polymer powders.

Finer particles are required for high-resolution laser sintering parts. Yet their advantages fall flat if powder flowability degrades to a point where it negatively impacts the process or the powder gets entirely unprocessable. In order to mitigate this, it is necessary to understand during which step of the powder application process it fails and the reason for it, in order to subsequently solve the issue by selectively improving other powder parameters, which is what this work is investigating.

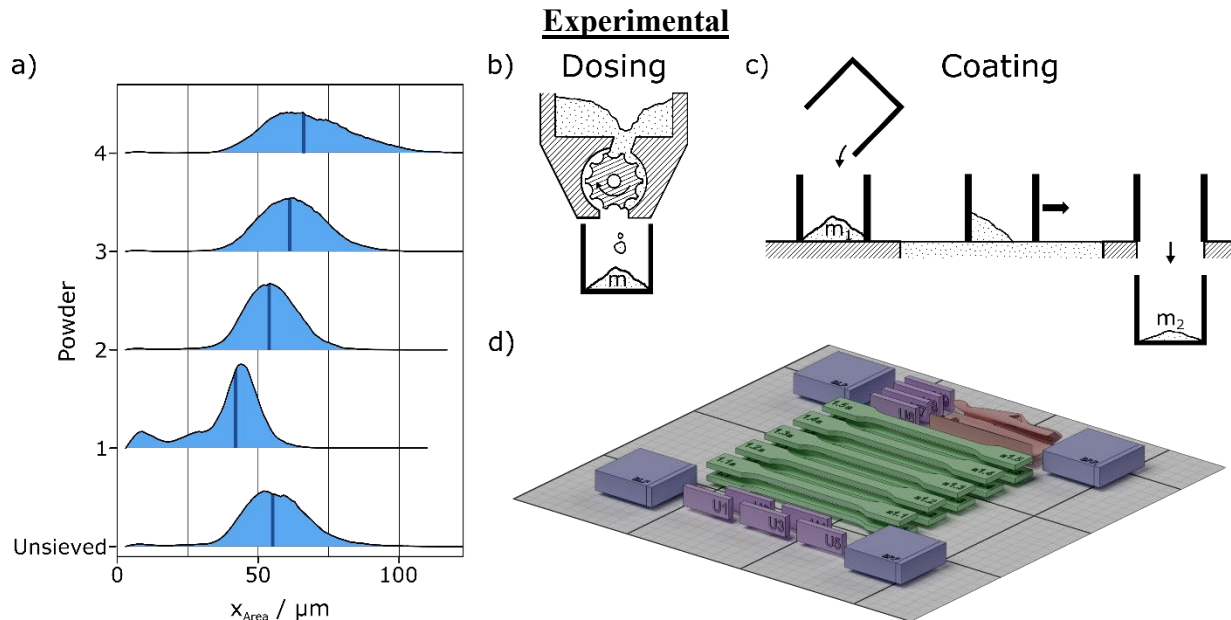


Fig. 1 a) Powder size distribution of the tested PA12 powder fractions, the blue line representing the d_{50} . Four powders, which were fractionated by sieving, and the original unsieved powder were

tested. b) and c) Schematic of isolated dosing and coating experiments on an EOS P395. d) Schematic representation of build job including tensile bars (green), powder boxes (blue), part density cuboids (purple) and a freeform part (red).

Material

A polyamide 12 (PA12) powder without any added flow agent was used for the following experiments.

Powder fractionation

Four powder fractions with different grain size distributions were created by sieving using an air-jet sieve (SLS 200, Siebtechnik GmbH, Germany). During sieving, static neutralizing bars (MEB, SIMCO B.V. Netherlands) were used to facilitate sieving. Sieves with mesh sizes of 80 μm , 63 μm and 40 μm were used.

Analytics

Powder rheology was determined by measuring the compression, aeration and unconfined yield strength on an FT4 powder rheometer (Freeman technology, Great Britain). The shearing measurements were done according to ASTM D7891-15. Pre-shear normal stress was set to 15kPa. The avalanche angle was measured with a Revolution Powder Analyzer (Mercury Scientific Inc., USA). 250 Avalanches were measured per sample at a rotation speed of 0.5 RPM and an inner drum diameter of 100 mm. Part density of the sintered cuboids was measured according to the Archimedes principle with a 770-60 scale (KERN & SOHN GmbH, Germany) in deionized water with a drop of dishwasher soap to decrease the surface tension of water. Tensile testing was done at norm conditions and according to DIN EN ISO 527-1:2019 employing a Zwick Z005 (ZwickRoell GmbH & Co. KG, Germany).

Dosing experiment

To investigate the dosing behavior of different powder fractions, this step was tested separately on a laser sintering machine (EOS P395, EOS GmbH, Germany). The powder was placed in the dosing bin 16h before the experiment. Fluidization in the dosing bin was set to 10 l/min in pulsed operation mode. 2 kg of powder were put in the dosing bin and conditioned for one hour with the fluidization turned on before starting the measurement. For each data point 10 units were dosed. One dosing unit is defined by the machine and corresponds to a theoretical maximum of 9.9 cm^3 . The dosed powder was collected and weighed with a scale, model WEJ 3000-2 (KERN & SOHN GmbH, Germany). This experiment was repeated 30 times for each of the 4 powder fractions as well as the unsieved powder. To minimize variation of powder settling due to the pulsed operation of fluidization, dosing was always done 5-10 s after fluidization had finished.

Coating experiment

Powder coating was tested by manually filling either 12.5g (referred to as “low filling”), 25 g (“normal filling”) or 37.5 g (“high filling”) of powder in the empty recoater, where the amount of 25 g was chosen such, that the recoater filling corresponded to the usual filling in a standard building process. The recoater was moved over the powder bed at a speed of 150 mm/s once and the remaining powder in the recoater was collected and weighed. The difference in weight, was assumed to be the powder deposited. The amount deposited was recorded 5 times for consecutive single layers. When changing recoater filling level, two layers were laid down unrecorded to reach equilibrium. It was verified afterwards, that an equilibrium had been reached. The measurement

was performed at room temperature, as well as at a temperature of 175°C, which is close to the process temperature for PA12. For the experiments at 175 °C, the powder was preheated to 70°C for 2h in an oven under N₂ atmosphere to account for the warming of the powder bin during the build process. The powder movement in the recoater during the coating steps was recorded with a GoPro Hero 7 (GoPro Inc., USA) mounted on the recoater.

Job setup

The build job is shown in Fig. 1 d). It includes 10 tensile bars in XY-direction according to DIN EN ISO 20753 type A1, 10 cuboids for determination of part density, 4 hollow boxes to measure the powder bed density and a freeform part for surface evaluation.

Build

The build was performed on an EOS P395 (EOS GmbH, Germany, Software: PSW 3.6.91) laser sintering machine, employing the PA2221_120_000 Default-Job, with the PA12 powder fractions described above and the reference powder. A temperature search determined the optimal build temperature to be 179°C. In all cases a 6 mm powder layer was laid down before preheating the machine for 2 hours prior to the job start. The powder in the dosing bin was fluidized in pulsed operation mode with a gas flow of 10 l/min. The build job was closely monitored and in case of an underfeed, more powder was added manually in order to avoid a build interruption.

Results and discussion

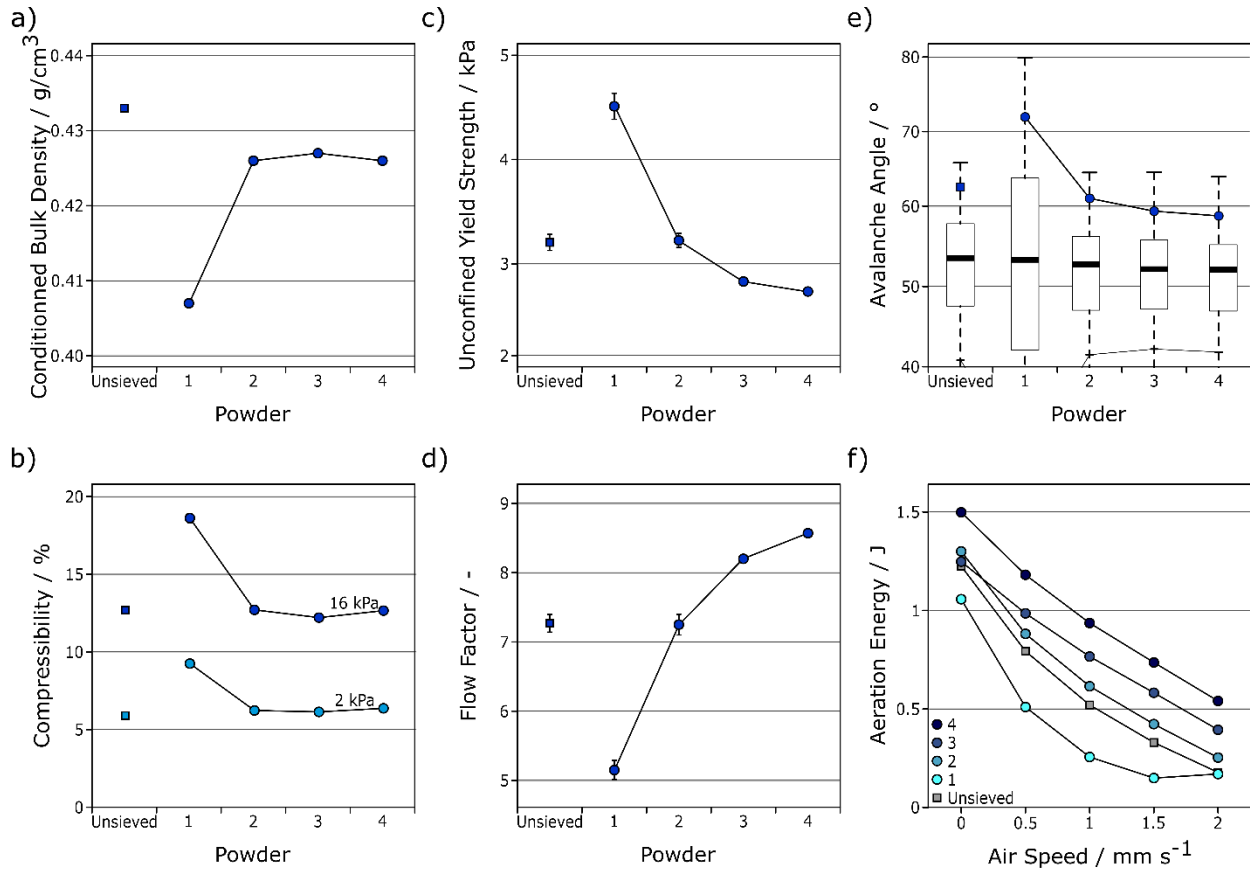


Fig. 2 a/b) Conditioned bulk density, and compressibility at both 2 and 16 kPa pressure, of the different powder fractions. c/d) Unconfined yield strength and the inversely behaving flow factor measured with a pre-shear normal stress of 15 kPa. e) The avalanche angle with the 95th percentile emphasized. f) Cumulative energy for a preset stirring program over fluidization flow.

The avalanche angle was measured at a slower speed than the speed of powder movement one would expect inside the recoater. Yet, with no normal stress on the powder, the powder flow conditions should be close to process behavior. As the avalanche angle is not a specific value, but rather a distribution (which in fact is not an inaccuracy of the measurement but a significant effect of the powder), not the median of each powder, but the 95th percentile was compared. It describes the angle of the powder surface at which an avalanche has reliably started. Considering the 99th percentile or largest recorded value would have been too prone to inconsistencies. Powders 2,3 and 4 had slightly increasing avalanche angles with finer powder distributions, but have had most avalanches by 60°, while powder fraction 1 had the 95th percentile at 71° with the last avalanches only breaking at 80°. Rheological behavior of the unsieved powder in all measurements is very similar to the powder fraction 2 which has a similar median value, but slightly narrower grain size distribution.

Contrary to the other measurements that had better flowability with larger particles, aeration of powders with finer particles was easier facilitated by the larger surface to mass ratio. Powder fraction 1 with the largest cohesion was easiest to fluidize and the only powder to reach an equilibrium within the range of the measurement. Weirdly, stirring energy for this powder was also

smallest with no air speed, despite its highest cohesion. This effect could be caused by the inferior powder packing behavior of this powder fraction.

Dosing

Dosing of the different powder fractions showed three effects (Fig. 3a). The amount of powder dosed decreased with increasing iterations for all powders. This can be attributed to the observed powder build-up on the dosing rolls which effectively reduced the volume each dosing unit can convey. Only powder fraction 1 reached an equilibrium during the experiment, yet at a pretty low level of around 10 g/iteration. The increased caking behavior of fraction 1 is in accordance with the higher compressibility and larger unconfined yield strength. This means, that under pressure the powder tends to rearrange more and the resulting powder cake is more stable.

Fractions 2-4 and the unsieved fraction showed similar behavior to each other during the whole experiment. The finest powder fraction 1 started at a lower level and quickly reached an equilibrium with significant fluctuation at roughly 10 g/10 dosing units, which is roughly a third of what the other powders started with and only around 25% of the theoretical maximum of roughly 40 g/10 dosing units (with a bulk density of PA12 of 0,41 g/cm³ (Fig. 2b)).

Two of the powder fractions (1 and 2) showed a dip in dosing at step 5 and 6. These were caused by bridging of the powder which had compacted over time during the resting phase before the experiment. The powder in the parallel gap between the bridge and the powder roll could still be dosed, before the powder bridge became problematic. Bridging could be solved by hitting the dosing bins, visibly collapsing the powder bridge. The reason, that the dip of powder fraction 1 did not go to near-zero was a result of the powder bin being hit when the effect was clearly visible, breaking powder bridges and, hence continuing the experiment. No significant caking or powder build-up was observed during later build jobs with any of the powders. This was probably prevented by the increased temperature and dry conditions during the building process.

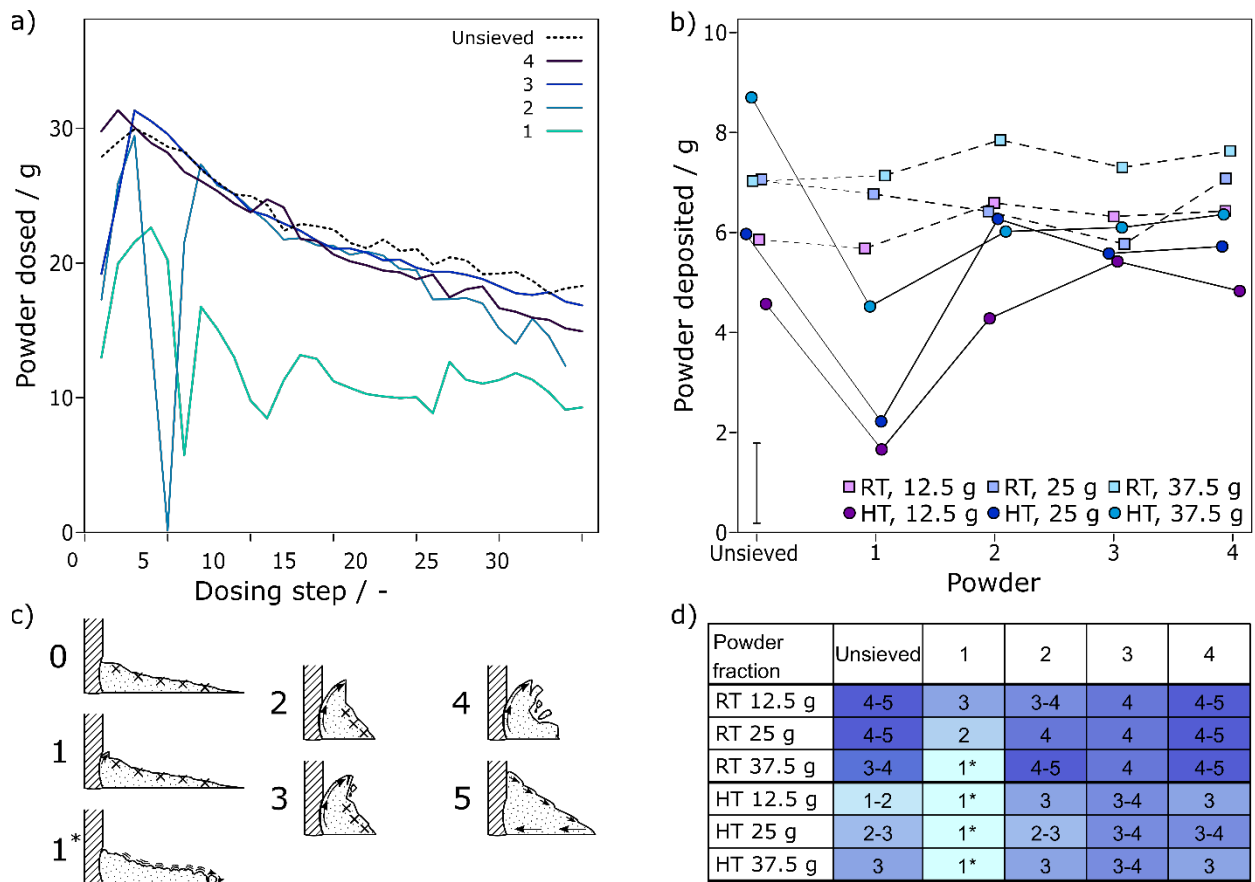


Fig. 3 a) Stability of the amount of powder dosed during subsequent steps of 10 dosing units, depending on the grain size distribution b) The amount of powder deposited on the powder bed depending on the grain size distribution and filling level of the recoater. This experiment was performed at room temperature (RT) as well as at operating temperature of 175 °C (HT). c) Classification of different powder movement behaviors in the recoater. 0: No visible powder movement. 1: Only slight scooping at the blade. 1*: No circulation, but rolling of agglomerates leading to visible vibrations. 2: Scooping motion without breaking. 3: As 2 but with chunks breaking off. 4: Circulation with chunks falling off regularly. 5: Near-continuous powder movement with small avalanches. d) Classification of the powder movement according to c) for the different experiments at room temperature (RT) and elevated temperature (HT) with a variation in recoater filling rate, dependent on the powder fraction.

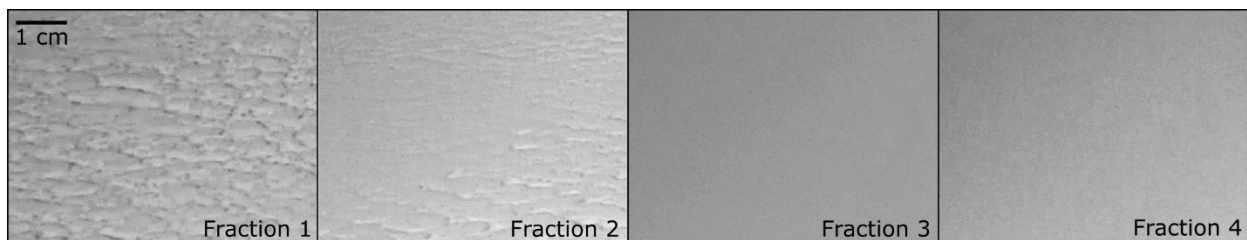


Fig. 4 Powder bed quality produced from the powder fractions at 175°C with 25g powder in recoater.

Coating

The amount of powder deposited in one coating step was measured for different powder fractions and recoater filling levels (Fig. 3b). This experiment was done at room temperature and at process temperature. In general, less powder was deposited at process temperature than at room temperature. Moreover, at room temperature, the amount of powder deposited was largely the same for all powder fractions, including the notoriously static fraction 1. Yet, a fuller recoater deposited slightly more powder. This was different, though, when repeating the experiment at operating temperature. Still, a fuller recoater had a positive influence on the amount of powder deposited, but additionally there was a difference between the five powder fractions. While of the powder fractions 2-4, which already showed very similar avalanche angles and similar unconfined yield strengths, also similar amounts of powder were deposited, powder fraction 1 performed significantly worse and only a third of the powder compared to the other fractions was deposited in the case of a normal recoater filling level of 25 g. A high filling level could partially mitigate this problem for this powder fraction. The unsieved powder behaved similar to the coarser powder fractions, except for the high filling level at operating temperatures which had two outliers with a large deposition, facilitated by an uneven powder bed.

Of special interest is the comparison of the amount of powder deposited in the different cases and the powder movement in the recoater (Fig. 3c/d). At room temperature all powders showed powder movement in the recoater. This was mostly independent of the filling level, except for fraction 1. This fraction showed less movement with a fuller recoater with only vibrations visible on the surface in the worst case and agglomerates being rolled between the powder and the powder bed. At operating temperatures, powder movement was generally reduced. The coarser powder fractions still showed adequate movement, but the finest fraction showed no powder movement anymore, rather agglomerates rolled as whole entities. As the powder mainly consisted of larger agglomerates, a thin layer of powder could not be coated. It is assumed that instead powder was scraped off of the agglomerates where it touched the powder bed, resulting in some deposition. Meanwhile slight irregularities, where the agglomerates did not contact the powder bed, resulted in no powder being deposited at all, which added up to grooves in the powder bed that got deeper with every layer (Fig. 4). The high recoater filling level of powder fraction 1 could partially mitigate this problem by more pressure on the powder bed under the powder's own weight. The behavior of the unsieved reference powder was somewhere in between the coarse and the fine fractions. In the case of a low filling level the powder seemed to float over the powder bed with no interaction at all, and only with more weight pushing down the powder a movement could be introduced. Overall, powders that showed powder movement of type 2 or lower resulted in a textured powder bed. More powder movement in the recoater led to a good powder bed (Fig. 4).

Build

The reference powder as well as the three coarser powders were adequately processable. While in single coating tests, coating of powder fraction 1 was successful and data could be obtained, process behavior was by far insufficient for a build job. The reduced powder dosage resulted in a constant underfeed which had to be counteracted by irregular extra dosing units. The bad coating behavior at operating temperatures then led to grooves in the powder bed in which the exposed parts would not result in a coherent part. These reasons quickly resulted in an entire job crash. Hence, unfortunately no mechanical properties could be determined of this powder. This was already indicated by analytical measurements, which showed a significantly inferior rheological behavior which was clearly visible in the dosing and coating experiments.

The powder bed density, as seen in Fig. 5a), shows the same trend as the conditioned bulk density, where the three powder fractions had a similar density. Meanwhile the unsieved powder showed a higher powder bed density, though this effect was stronger than the conditioned bulk density suggested. Part density of the cuboids and Young's modulus both showed a slightly increasing trend with coarser powder fractions and the unsieved powder being roughly in the middle, and for the Young's modulus with a larger standard deviation. The difference between the trends of powder bed density and part density, could be explained by the fact that in a powder bed the grains need to pack with solid particles, hence the good correlation with the conditioned bulk density measurement. Yet, in a part the new powder is being pressed into the underlying still molten layer. The differences between the part density and Young's modulus are minor though, but in the case of the part density still larger than the standard deviation. They could show a tendency of part density and Modulus being influenced by the increasing bulk density of the fractions but could also be caused by variations in-between different builds. Elongation at break was not significantly different for the powders that were processable.

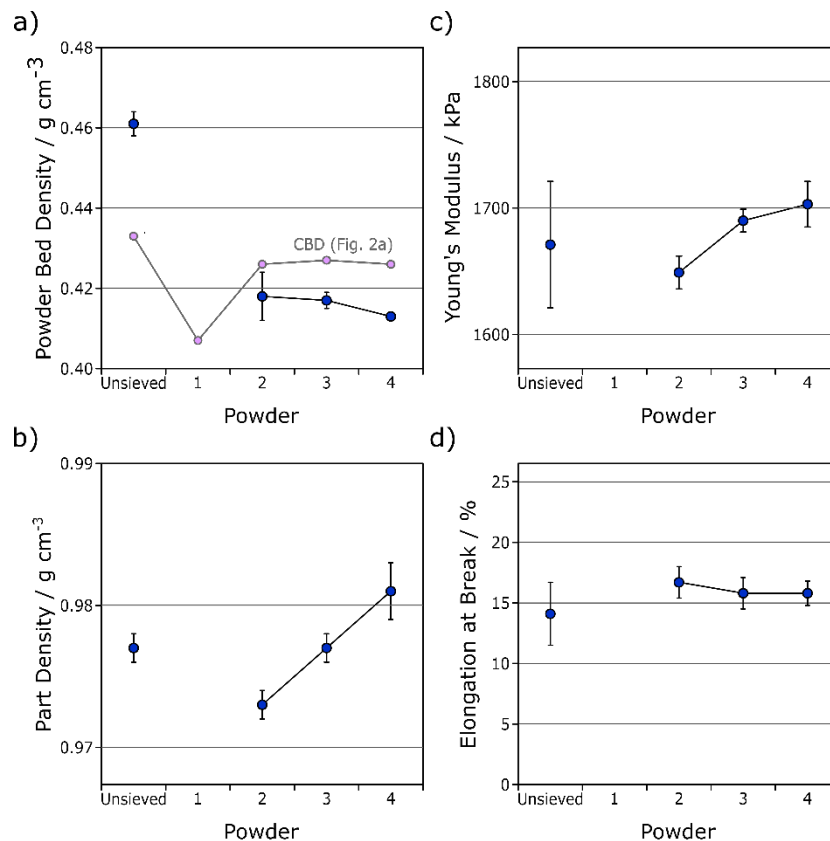


Fig. 5 Data gathered from the test parts of the build jobs. Data points for fraction 1 have been left empty as the fraction could not be processed. a) Powder bed density in measured from powder enclosed in hollow parts. b) Part density of test parts. c/d) Mechanical properties of tensile bars.

It is unfortunate, that the powder fraction 1 performed so much worse than the other powder fractions and could not be processed. Nevertheless, the builds jobs indicate, that the better flowability of coarser powder fractions result in slightly improved part density and stiffness. As the experiments were not repeated, this effect could be coincidental. More importantly, it could be shown that the fines define the powder behavior significantly more than the average grain size. On

the positive side, this does indicate, that finer powder fractions, than are currently common, can still yield promising results, as long as the finest fraction is removed, especially when flow additives are added to the powders. The presented experiments were performed without any flow agents, which are commonly used in laser sintering materials. This means, that powders are expected to perform significantly better when flow agent is being added. Moreover, it can be assumed, that it is viable for powders with finer grain size distribution to perform well for laser sintering and other powder bed fusion processes.

Conclusion and Outlook

This work showed the influence of particle size distribution on powder rheology through different steps of the powder application process on a laser sintering machine as well as the influence on properties of test specimens built. A standard PA12 powder was sieved into 4 fractions with different particle size distributions. It could be shown that the bulk density of powder fractions with a narrower particle size distribution was slightly lower than for the unsieved powder with a wider particle size distribution. This can be explained by a better packing due to filling up gaps with smaller particles. The results from fraction 1 (<40 μm) showed impressively the influence of the finest fraction of particles. Here, obviously intermolecular interactions and attraction dominate the powder rheology and lead to a powder which behaves sticky and tends to build agglomerates.

The differences in powder rheology were transferable to the consecutive process steps of powder application in the laser sintering machine, where the fine fraction had the highest tendency for bridging in the dosing system and showed little movement in the recoater. The dosing behavior was in line with the results from the unconfined yield strength and compressibility measurements. Comparing the coating process with the resulting properties of the test specimens indicated that the movement in the recoater is critical for the creation of a smooth and dense powder bed which again is inevitable for dense parts with decent mechanical properties. The powder movement inside the recoating system correlated well with the analytical measures determined from shear-cell, powder rheometer and the Revolution Powder Analyzer, which therefore can be employed to improve the prediction of powder processability based on powder analytics.

Acknowledgements

The authors acknowledge Prof. Katrin Wudy (Professorship of Laser-based Additive Manufacturing; TUM) for supervising Mr. Riedmann's project and the insightful discussions.

References

- [1] P. B. Bacchewar, S. K. Singhal and P. M. Pandey, "Statistical modelling and optimization of surface roughness in the selective laser sintering process," *Proceedings of the Institution of Mechanical Engineers, Part B: Journal of Engineering Manufacture*, vol. 221, pp. 35-52, 2007.
- [2] S. Ziegelmeier, P. Christou, F. Wöllecke, C. Tuck, R. Goodridge, R. Hague, E. Krampe and E. Wintermantel, "An experimental study into the effects of bulk and flow behaviour of laser sintering polymer powders on resulting part properties," *Journal of Materials Processing Technology*, vol. 215, no. 1, pp. 239-250, 2015.
- [3] M. J. Krantz, H. Zhang and J. Zhu, "Characterization of powder flow: Static and dynamic testing," *Powder Technology*, vol. 194, pp. 239-245, 2009.
- [4] T. Köhler and H. Schubert, "Influence of the Particle Size Distribution on the flow behaviour of fine powders," *Particle & Particle Systems Characterization*, vol. 8, no. 1-4, pp. 101-104, 1991.
- [5] K. Thalberg, D. Lindholm and A. Axelsson, "Comparison of different flowability tests for powders for inhalation," *Powder Technology*, vol. 146, pp. 206-213, 2004.
- [6] H. P. Goh, P. W. S. Heng and C. V. Liew, "Comparative evaluation of powder flow parameters with reference to particle size and shape," *Int J Pharm*, vol. 542, no. 1-2, pp. 113-141, 2018.
- [7] X. Fu, D. Huck, L. Makein, B. Armstrong, U. Willen and T. Freeman, "Effect of particle shape and size on flow properties of lactose powders," *Particuology*, vol. 10, no. 2, pp. 203-208, 2012.
- [8] H. Shi, R. Mohanty, S. Chakravarty, R. Cabisco, M. Morgeneyer, H. Zetzener, J. Y. Ooi, A. Kwade, S. Luding and V. Magnanimo, "Effect of Particle Size and Cohesion on Powder Yielding and Flow," *KONA Powder and Particle Journal*, pp. 226-250, 2018.
- [9] L. Meyer, A. Wegner and G. Witt, "Influence of the Ratio between the Translation and Contra-Rotating Coating Mechanism on different Laser Sintering Materials and their Packing Density," in *Solid Freeform Fabrication 2017*, Austin, 2017.
- [10] A. Averardi, C. Cola, S. E. Zeltmann and N. Gupta, "Effects of particle size distribution on the packing of powder beds: A critical discussion relevant to additive manufacturing," *Materials Today Communications*, vol. 24, no. 2352-4928, p. 100964, 2020.

- [11] N. P. Karapatis, G. Egger, P. Gygax and R. Glardon, "Optimization of powder layer density in selective laser sintering," in *International Solid Freeform Fabrication Symposium*, Austin, 1999.
- [12] A. W. Jenike, "Storage and flow of solids," *Bulletin No. 123 of the Utah Engineering Experiment Station*, vol. 53, no. 26, 1976.